Single subcutaneous injection of a pyrrolizidine alkaloid, namely, monocrotaline (MCT), produces severe PAH and PA remodeling in rats. We examined the effects of sustained PGIS expression in preventing PAH development and progression by means of this widely used model and an AAV1 vector.

Methods

Western Blot Analysis for PGIS Expression In Vitro

Human embryonic kidney 293 (HEK293) cells were incubated in 10-cm dishes containing DMEM and nutrient mixture F12 (Invitrogen) with 2% FCS in an atmosphere of 5% CO_2 in air at 37°C. The cells at 70% confluence were transfected with an AAV proviral plasmid encoding human PGIS (phPGIS, a kind gift from Dr Mimuro) or plasmid encoding enhanced green fluorescent protein (eGFP) by using a calcium phosphate method. The cells were harvested 72 hours after transfection, and cell lysates were prepared with a lysis buffer (10 mmol/L of Tris-HCl, 150 mmol/L of NaCl, and 1% NP40 [pH 7.6]) containing Complete Mini protease inhibitor (Roche Diagnostics). For Western blot analysis, 10 μg of the lysate was subjected to 10% SDS-PAGE and transferred to a nitrocellulose membrane. The membrane was blocked and incubated with a 1:500 dilution of rabbit anti-human PGIS polyclonal antibody (a gift from Dr Mimuro) and a 1:5000 dilution of peroxidase-linked anti-rabbit IgG antibody (Amersham Pharmacia Biotech), and immunoreactive bands were visualized using an enhanced chemiluminescence Western blotting kit (Amersham).

AAV-PGIS Production and PGI_2 Expression

We developed a recombinant AAV1-based vector containing the human PGIS or eGFP gene controlled by a modified chicken β-actin promoter with a cytomegalovirus immediate-early enhancer (AAV-PGIS or AAV-eGFP) to obtain efficient transgene expression in skeletal muscle cells. The AAV vectors were prepared according to the previously described 3-plasmid transfection adenovirus-free protocol with minor modifications for enabling the use of an active gassing system.[10,11] In brief, 60% confluent HEK293 cells that were incubated in a large culture vessel with active air circulation were cotransfected with phPGIS, AAV-1 chimeric helper plasmid (p1RepCap), and adenoviral helper plasmid pAdeno (Avigen Inc). The crude viral lysate was purified with 2 rounds of cesium chloride 2-tier centrifugation.[12] The titer of the viral stock was determined against plasmid standards by real-time PCR with primers 5′-CCCGCGAGGTTGTGGTGGAC-3′ and 5′-ATGGGCGGATGCGGTAGC-3′; subsequently, the stock was dissolved in a buffer (50 mmol/L of HEPES [pH 7.4] and 0.15 mol/L of NaCl [HN buffer]) before infection. The HEK293 cells cultured in 6-well plates containing DMEM and nutrient mixture F12 with 5% FCS were infected with AAV-PGIS at 1×10^4 genome copies per cell to evaluate PGI_2 expression in vitro, and the supernatant was harvested after 72 hours. Concentrations of 6-keto-prostaglandin $F_{1\alpha}$ (6-keto-$PGF_{1\alpha}$) in plasma or culture media were determined by enzyme immunoassay (R&D Systems) according to the manufacturer's instructions. The minimum detectable dose of the assay was <1.4 pg/mL. Interassay and intra-assay precision of the kit was <10%.

Animal Models

All of the animal experiments were approved by the Jichi Medical University ethics committee and were performed in accordance with the National Institutes of Health Guide for the Care and Use of Laboratory Animals. To evaluate the efficiency of gene expression in vivo, AAV-eGFP (200 μL; 1×10^{11} gene copies per body) or AAV-PGIS (200 μL; 1×10^{10} to 1×10^{11} gene copies per body) was injected into the bilateral anterior tibial muscles (n=3 each) of 3-week–old male Wistar rats (Clea Japan Inc) weighing 45 to 55 g. For hemodynamics and histological analyses, the rats were divided into 4 groups: sham rats that were administered the HN buffer (group 1, negative control [NC] group; n=4); MCT-PAH rats administered the HN buffer (group 2, MCT group; n=6); MCT rats administered AAV-eGFP (group 3, MCT+eGFP group; n=6); and MCT rats administered AAV-PGIS (group 4, MCT+PGIS group; n=10). After the anesthesia with spontaneous inhalation of 1% isoflurane, the rats in groups 3 and 4 were intramuscularly injected with AAV-eGFP or AAV-PGIS (1×10^{10} gene copies per body), whereas those in groups 1 and 2 were injected with the HN buffer (200 μL). MCT (Wako Pure Chemicals) was dissolved in 0.1 N HCl, and the pH was adjusted to 7.4 with 1.0 N NaOH. After the anesthesia with spontaneous inhalation of 1% isoflurane, all of the rats except for those in the NC group were injected subcutaneously with MCT (40 mg/kg) 4 weeks after the injecting the vector. Blood samples were collected from the tail vein on ethylenediamine tetraacetic acid tubes, and the concentrations of the leukocytes, platelets, hematocrit, alanine aminotransferase, and creatinine were determined by standard procedures.

Hemodynamics Analysis

Four weeks after the MCT injection, the rats were anesthetized with spontaneous inhalation of 1% isoflurane, and a tracheotomy was performed. Then, they were mechanically ventilated with 1% isoflurane (tidal volume, 10 mL/kg; respiratory rate, 30 breaths per minute) through a tracheostomy. After the thoracic cavity was opened using a midsternal approach, 2F high-fidelity manometer-tipped catheters (SPC-320; Millar Instruments Inc) were inserted directly into the right or left ventricle, and an ultrasonic flow probe (flow probe 2.5S176; Transonic Systems Inc) was placed on the ascending root of the aorta. The heart rate, mean pulmonary arterial pressure (mPAP), aortic systolic arterial pressure, left ventricular end-diastolic pressure (LVEDP), and mean aortic flow indicating the cardiac output (CO) were measured. Cardiac indices (CI) and pulmonary vascular resistance (PVR) were calculated using the following formula: $CI\ (mL\cdot min^{-1}\cdot kg^{-1})=CO/body\ weight$, $PVR\ (mm\ Hg\cdot mL^{-1}\cdot min^{-1}\cdot kg^{-1})=(mPAP-LVEDP)/CI$.

Ventricular Weight Measurement and Morphometric Analysis of the PA

After the hemodynamic analysis, the rats were killed with an overdose (5%) of isoflurane through a tracheostomy. Their lungs were perfused with 5 mL of saline followed by 10 mL of cold 4% paraformaldehyde. Each ventricle and the lungs were then excised, dissected free, and weighed. The weight ratio of the right ventricle to the left ventricle plus septum [RV/(LV+S)] was calculated as an index of right ventricular hypertrophy (RVH). The lung tissues were fixed overnight at 4°C in 4% paraformaldehyde and frozen in Tissue-Tek OCT compound (Sakura Finetechnical Co) at −20°C. Hematoxylin and eosin staining was performed on 7-μm–thick sections that were subsequently examined using light microscopy. A morphometric analysis was performed on a PA having an external diameter of 25 to 50 μm or 51 to 100 μm. The medial wall thickness was calculated using the following formula: medial thickness (%)=medial wall thickness/external diameter×100.[13] For the quantitative analysis, 30 vessels of each rat were measured and averaged randomly by the 2 external observers.

Survival Analysis

The 3-week–old Wistar rats were divided into 3 groups (MCT, MCT+eGFP, and MCT+PGIS; n=8 each). After the anesthesia with spontaneous inhalation of 1% isoflurane, the rats in the MCT+eGFP or MCT+PGIS group were intramuscularly injected with AAV-eGFP or AAV-PGIS at 1×10^{10} genome copies per body, respectively. Under the same anesthetic condition, all of the rats were injected subcutaneously with MCT (40 mg/kg) at 4 weeks after injecting the vector. The survival rate was estimated from the date of the MCT administration until death or after 8 weeks of the injection. Survival curves were analyzed using the Kaplan-Meier method and compared by log-rank tests.

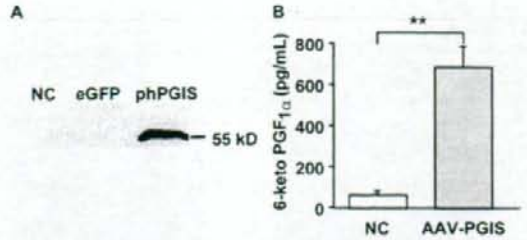

Figure 1. Expression of PGIS and PGI_2 in vitro. A, Western blot analysis of PGIS expression in HEK293 cells after plasmid transfection. The cells were harvested 72 hours after transfection with phPGIS or eGFP. B, AAV vector-mediated PGI_2 expression in HEK293 cells. The PGI_2 levels were estimated by measuring the amount of 6-keto-$PGF_{1\alpha}$, a stable metabolite of PGI_2, in the culture supernatant by enzyme immunoassay 72 hours after infecting the cells (n=4 each) with AAV-PGIS (1×10^4 genome copies per cell). Data are presented as mean±SEM. $^{**}P<0.01$. NC indicates untreated negative control.

Statistical Analysis

The statistical analysis and correlations were performed using StatView (Abacus Concepts, Inc). Data are presented as mean±SEM. Differences in parameters were evaluated using ANOVA combined with Fisher's test. A value of $P<0.05$ was considered statistically significant.

Results

Expression of PGIS and PGI_2 In Vitro

Western blot analysis revealed that transfection of the HEK293 cells with phPGIS but not with a plasmid carrying the eGFP gene enhanced the production of the PGIS protein (Figure 1A). Infection of the cells with AAV-PGIS at 1×10^4 genome copies per cell significantly increased the concentration of 6-keto-$PGF_{1\alpha}$, a stable metabolite of PGI_2, in culture supernatants as compared with that without vector infection (Figure 1B).

AAV Vector-Mediated Systemic PGI_2 Expression in the Rats

Four weeks after the injection of AAV vectors (1×10^{10} genome copies per body), the PGIS-transduced rats began exhibiting significant increases in the plasma 6-keto-$PGF_{1\alpha}$ levels as compared with the control rats (Figure 2A). Eight weeks after the injection, the 6-keto-$PGF_{1\alpha}$ levels increased further in a vector dose-dependent manner in the treated rats (Figure 2B) as compared with the untreated controls (6.68±1.33 versus 1.62±0.30 ng/mL, 1×10^{11} versus 1×10^{10} genome copies per body, respectively; $P<0.05$; n=3 each). The vectors at 1×10^{10} genome copies per body were used for all of the subsequent experiments. In contrast, injection of 1×10^{11} genome copies per body of AAV-eGFP produced no significant change in the 6-keto-$PGF_{1\alpha}$ levels.

Effects of PGI_2 Expression on Hemodynamics and RVH

Four weeks after the MCT administration, the mPAP levels were significantly elevated in the treated rats as compared with the untreated controls (Figure 3A). Treatment with AAV-PGIS but not AAV-eGFP significantly inhibited this increase (Figure 3A). In addition, the expression of PGI_2

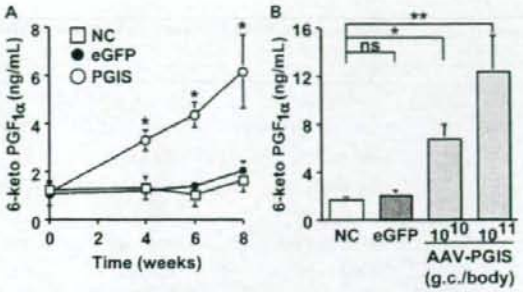

Figure 2. AAV vector-mediated systemic expression of PGI_2 in vivo. The concentration of plasma 6-keto-$PGF_{1\alpha}$ was determined by enzyme immunoassay after a single injection of AAV-PGIS into the anterior tibial muscle of 3-week-old male Wistar rats. A, Time course of plasma 6-keto-$PGF_{1\alpha}$ levels after injection of AAV-PGIS at 1×10^{10} genome copies per body. B, Vector dose dependency of plasma 6-keto-$PGF_{1\alpha}$ levels 8 weeks after the injection. The rats injected with AAV-eGFP (1×10^{11} genome copies per body) were used as controls. Data are presented as mean±SEM (n=3 animals per group). ns indicates not statistically significant; NC, untreated negative control. $^{*}P<0.05$ vs NC; $^{**}P<0.01$.

significantly mitigated an increase in PVR and a decrease in CI that were induced by MCT (Figure 3B and 3C, respectively); however, it produced no significant changes in the heart rate and aortic systolic arterial pressure (Table). PGI_2 expression also had a beneficial effect on RVH. Treatment with AAV-PGIS but not AAV-eGFP significantly inhibited the MCT-induced increase in RV/(LV+S) (Figure 3D).

Effects on Medial Hypertrophy of the PA

Medial hypertrophy is a hallmark of pathological vascular remodeling in PAH. Four weeks after the MCT injection, the

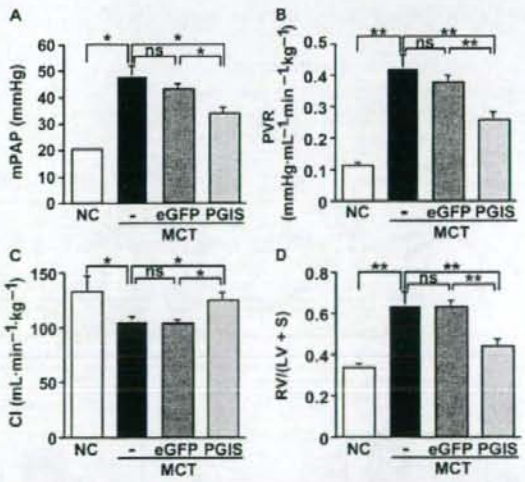

Figure 3. Effects of PGI_2 on hemodynamics and RVH. A quantitative analysis was performed using MCT-induced PAH rats 8 weeks after injecting the vector. A, mPAP (mm Hg); B, PVR (mm Hg · mL^{-1} · min^{-1} · kg^{-1}); C, CI (mL · min^{-1} · kg^{-1}). D, Weight ratio of the right ventricle to the left ventricle plus septum [RV/(LV+S)] presented as an index of RVH. Data are presented as means±SEM (n=4 to 10 animals per group). $^{*}P<0.05$; $^{**}P<0.01$. ns indicates not statistically significant; NC, untreated negative control.

Physiological and Laboratory Data of the MCT-Induced PAH Rats

Factor	NC	MCT	MCT+eGFP	MCT+PGIS	*P*
No. of rats	4	6	6	10	...
Heart rate, per minute	294.0±10.6	281.2±14.7	268.0±9.0	274.8±8.7	NS
ASAP, mm Hg	99.5±1.6	97.3±2.0	96.3±2.4	94.7±4.4	NS
Body weight, g	358.5±11.5	328.3±7.2	328.0±11.4	342.5±9.8	NS
Leukocyte, per mL	6725±372	7917±723	8800±849	8030±852	NS
Hematocrit, %	48.2±0.7	48.9±1.9	51.0±3.0	47.8±1.8	NS
Platelet, $\times 10^4/mm^3$	88.3±8.7	79.2±8.8	80.4±3.6	84.6±6.3	NS
ALT, IU/L	37.8±2.5	49.5±8.4	52.5±6.8	44.1±4.3	NS
Cr, mg/dL	0.52±0.04	0.59±0.05	0.48±0.03	0.53±0.04	NS

Data are presented as means±SEM (n=4 to 10 animals per group). ASAP indicates aortic systolic arterial pressure; ALT, serum alanine aminotransferase; Cr, serum creatinine; NS, not statistically significant.

medial thickness of the PA was greater in the MCT-administered rats than in the untreated controls (Figure 4A). Treatment with AAV-PGIS but not AAV-eGFP prevented the MCT-induced increase in the percentage of medial thickness significantly (Figure 4B, 25 to 50 μm; Figure 4C, 51 to 100 μm in external diameter).

Effects on the Survival of the MCT-PAH Rats and Their Organ Dysfunctions

The PGIS-transduced rats exhibited significantly improved survival rates as compared with the eGFP-transduced rats (Figure 5). The MCT administration produced a slight but not significant decrease in the body weight of the rats, and PGIS gene transfer prevented this decrease. Although the MCT group showed only a slight but not significant increase in the leukocyte count and serum alanine aminotransferase levels as compared with the NC group, the AAV-PGIS treatment caused no additional change in these parameters (Table).

Discussion

The present study demonstrates that sustained PGI_2 expression by a single intramuscular injection of AAV-PGIS prevents the development of MCT-PAH in rats. PGI_2 expression not only increased the cardiac output significantly but also prevented the progression of PVR, RVH, and medial hypertrophy of the PA that was induced by the MCT administration. The PGIS-transduced rats also exhibited significantly improved survival rates as compared with the controls. Furthermore, the PGIS expression observed in this study caused no additional adverse effects on hematologic data and serum indicators of hepatorenal function (alanine aminotransferase and creatinine levels) in the MCT-PAH rats.

The expression of PGI_2 and PGIS decreased in the remodeled PAs of the idiopathic PAH patients.[14,15] Impaired PGI_2 synthesis resulting from a decrease in PGIS expression may be implicated in the pathogenesis of PAH. In fact, continuous intravenous infusion of exogenous PGI_2 markedly lowers PVR and improves survival in PAH patients. However, this system requires lifelong infusion with a central venous catheter because of the short biological half-life of PGI_2. Furthermore, because this system is associated with life-threatening complications (eg, shock and sepsis) that may result in poor survival and quality of life of patients, stable

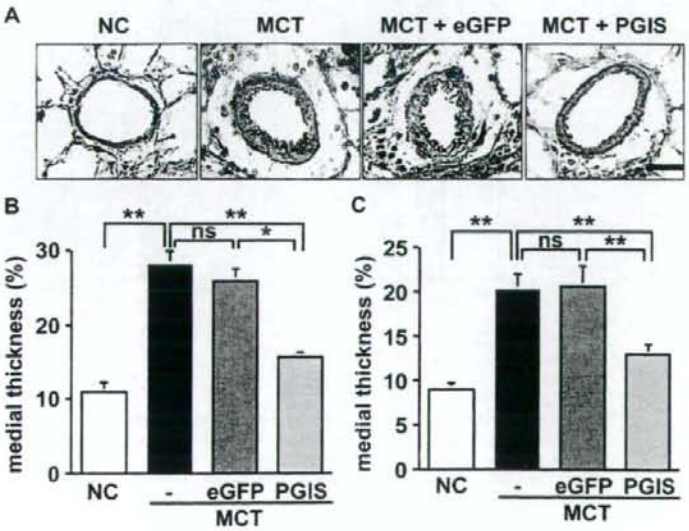

Figure 4. Effects of PGI_2 on medial hypertrophy of the peripheral PA. A, Representative cross-sections of the peripheral PA 4 weeks after the MCT administration (hematoxylin and eosin staining, original magnification, ×1000; scale bar=20 μm). B and C, Quantitative analysis of percentage of medial thickness (B, 25 to 50 μm; C, 51 to 100 μm in external diameter). Data are presented as means±SEM (n=4 to 10 animals per group). *P<0.05, **P<0.01. ns indicates not statistically significant; NC, untreated negative control.

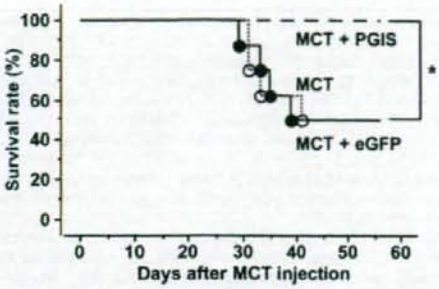

Figure 5. The survival rate of MCT-induced PAH rats. The rats were administered with MCT (40 mg/kg) 4 weeks after the injection of HN buffer (MCT group), AAV-eGFP (MCT+eGFP group), or AAV-PGIS (MCT+PGIS group). The rats were intramuscularly injected with the vectors at 1×10^{10} genome copies per body. The Kaplan-Meier method demonstrated a significant improvement in the survival rate of the rats in the MCT+PGIS group as compared with those in either the MCT or MCT+eGFP group at 8 weeks post-MCT administration. n=8 animals per group; *$P<0.05$ vs MCT or eGFP groups.

production of endogenous PGI_2 would be more desirable. Consistent with previous gene therapy studies, our strategy presented high levels of endogenous PGI_2 expression. In addition, this strategy caused no systemic hypotension and hyperdynamic heart failure, which are the major adverse effects arising from uncontrolled blood levels during intravenous delivery of exogenous PGI_2.[3,4,6]

In this study, we used an AAV serotype 1 vector because it is effective not only in efficient muscle transduction but also in long-term secretion of therapeutic proteins into the systemic circulation. The cDNA for human PGIS shares a high identity with its rat counterpart.[16] In fact, the administration of a plasmid or hemagglutinating virus of the Japan-liposome vector encoding human PGIS successfully ameliorated MCT-PAH. However, the use of these vectors requires repeated administration for achieving sustained gene expression.[3–5] In contrast, the AAV vector used in this study achieved PGIS expression with a single intramuscular injection, and this expression was sustained for 1 year.[7]

Furthermore, gene transfer was believed to be safer when performed via an intramuscular approach as opposed to the intratracheal or intrahepatic approaches.[6] Currently, researchers are using adenoviral gene transfer in most clinical trials because of its high efficiency for gene expression. However, the potential toxic effects of adenoviruses, such as strong immunogenicity, are well known. In contrast, the intramuscular administration of AAV vectors is a promising strategy for delivering therapeutic proteins safely and efficiently, and their use has been examined in clinical trials for hemophilia.[17]

Although PGI_2 is known to be a short-acting vasodilator, recent studies have shown its antiremodeling effects when used in high doses. The administration of PGI_2 analogues cicaprost and iloprost in high concentrations ($>10^{-7}$ mol/L) inhibits mitogen-induced proliferation of rat primary PA smooth muscle cells in a cAMP-dependent manner.[18] Interestingly, another PGI_2 analogue, treprostinil, also inhibits the proliferation of human and mouse primary lung fibroblasts through the activation of a peroxisome proliferator-activated receptor-β/δ when used in equivalent doses.[19] These observations suggest that high levels of PGI_2 may attenuate PA remodeling in vivo through antiproliferative effects. Consistent with previous studies, we demonstrated that high levels of endogenous PGI_2 successfully attenuated medial hypertrophy of the PA.[3,4,6] To discover new drug targets, the roles of peroxisome proliferator-activated receptors and high-level PGI_2 in PAH therapy should be determined, because peroxisome proliferator-activated receptors are associated with many inflammatory and proliferative disorders, including PAH.[2,20]

Finally, we will discuss the clinical implications and limitations of this study. Consistent with previous studies, maximum gene expression was noted 6 to 8 weeks after the intramuscular injection of AAV vectors. AAV-PGIS was injected 4 weeks before MCT administration for the transgene expression to reach plateau levels when MCT-PAH was fully developed (3 to 4 weeks after the injection). Our results are completely based on a preventive protocol, which may be rare in a clinical setting. However, PGI_2 is an established therapeutic molecule, and the advantage of early initiation of PGI_2 therapy for improving survival in patients with idiopathic PAH has been demonstrated in a large clinical trial.[21] These observations convinced us to propose the possible preemptive use of AAV-PGIS as a strategy to maintain basal levels of PGI_2 in patients with mild symptoms of PAH or in those identified as high-risk subjects who have not experienced PAH. As an alternative, the combined use of AAV-PGIS and an initial infusion of intravenous PGI_2 might be promising; the intravenous infusion should be tapered when sufficient levels of PGI_2 are attained. To evaluate the efficacy of AAV-PGIS in a therapeutic protocol (ie, vector injection after the development of PAH), use of a chronic hypoxic PAH model or newly developed self-complementary AAV vectors that can express transgenes earlier than the conventional vectors should be considered.[22]

Perspectives

The present study has demonstrated that the single intramuscular injection of AAV-PGIS achieved a sustained expression of PGI_2. This expression retarded the progression of MCT-PAH in rats without causing significant adverse effects. Thus, this strategy provides a new therapeutic alternative for PAH patients. However, the system in this study lacks the ability to regulate excessive transgene expression. Therefore, regulatory mechanisms to ensure adequate gene expression should be established to facilitate successful translation of this strategy in a clinical setting.

Acknowledgment

We thank Miyoko Mitsu for her encouragement and technical support.

Sources of Funding

This work was supported in part by grants from the Ministry of Health, Labor and Welfare of Japan; Grants-in-Aid for Scientific Research; grant for the 21st Century Centes of Excellence Program; "High-Tech Research Center" Project for Private Universities, matching fund subsidy, from the Ministry of Education, Culture,

Sports, Science and Technology of Japan; and the Research Award to Jichi Medical School Graduate Student.

Disclosures

None.

References

1. Humbert M, Sitbon O, Simonneau G. Treatment of pulmonary arterial hypertension. *N Engl J Med*. 2004;351:1425–1436.
2. Ito T, Ozawa K, Shimada K. Current drug targets and future therapy of pulmonary arterial hypertension. *Curr Med Chem*. 2007;14:719–733.
3. Nagaya N, Yokoyama C, Kyotani S, Shimonishi M, Morishita R, Uematsu M, Nishikimi T, Nakanishi N, Ogihara T, Yamagishi M, Miyatake K, Kaneda Y, Tanabe T. Gene transfer of human prostacyclin synthase ameliorates monocrotaline-induced pulmonary hypertension in rats. *Circulation*. 2000;102:2005–2010.
4. Suhara H, Sawa Y, Fukushima N, Kagisaki K, Yokoyama C, Tanabe T, Ohtake S, Matsuda H. Gene transfer of human prostacyclin synthase into the liver is effective for the treatment of pulmonary hypertension in rats. *J Thorac Cardiovasc Surg*. 2002;123:855–861.
5. Ono M, Sawa Y, Mizuno S, Fukushima N, Ichikawa H, Bessho K, Nakamura T, Matsuda H. Hepatocyte growth factor suppresses vascular medial hyperplasia and matrix accumulation in advanced pulmonary hypertension of rats. *Circulation*. 2004;110:2896–2902.
6. Tahara N, Kai H, Niiyama H, Mori T, Sugi Y, Takayama N, Yasukawa H, Numaguchi Y, Matsui H, Okumura K, Imaizumi T. Repeated gene transfer of naked prostacyclin synthase plasmid into skeletal muscles attenuates monocrotaline-induced pulmonary hypertension and prolongs survival in rats. *Hum Gene Ther*. 2004;15:1270–1278.
7. Yoshioka T, Okada T, Maeda Y, Ikeda U, Shimpo M, Nomoto T, Takeuchi K, Nonaka-Sarukawa M, Ito T, Takahashi M, Matsushita T, Mizukami H, Hanazono Y, Kume A, Ookawara S, Kawano M, Ishibashi S, Shimada K, Ozawa K. Adeno-associated virus vector-mediated interleukin-10 gene transfer inhibits atherosclerosis in apolipoprotein E-deficient mice. *Gene Ther*. 2004;11:1772–1779.
8. Chen S, Kapturczak MH, Wasserfall C, Glushakova OY, Campbell-Thompson M, Deshane JS, Joseph R, Cruz PE, Hauswirth WW, Madsen KM, Croker BP, Berns KI, Atkinson MA, Flotte TR, Tisher CC, Agarwal A. Interleukin 10 attenuates neointimal proliferation and inflammation in aortic allografts by a heme oxygenase-dependent pathway. *Proc Natl Acad Sci U S A*. 2005;102:7251–7256.
9. Mu W, Ouyang X, Agarwal A, Zhang L, Long DA, Cruz PE, Roncal CA, Glushakova OY, Chiodo VA, Atkinson MA, Hauswirth WW, Flotte TR, Rodriguez-Iturbe B, Johnson RJ. IL-10 suppresses chemokines, inflammation, and fibrosis in a model of chronic renal disease. *J Am Soc Nephrol*. 2005;16:3651–3660.
10. Matsushita T, Elliger S, Elliger C, Podsakoff G, Villarreal L, Kurtzman GJ, Iwaki Y, Colosi P. Adeno-associated virus vectors can be efficiently produced without helper virus. *Gene Ther*. 1998;5:938–945.
11. Okada T, Nomoto T, Yoshioka T, Nonaka-Sarukawa M, Ito T, Ogura T, Iwata-Okada M, Uchibori R, Shimazaki K, Mizukami H, Kume A, Ozawa K. Large-scale production of recombinant viruses by use of a large culture vessel with active gassing. *Hum Gene Ther*. 2005;16:1212–1218.
12. Okada T, Nomoto T, Shimazaki K, Lijun W, Lu Y, Matsushita T, Mizukami H, Urabe M, Hanazono Y, Kume A, Muramatsu S, Nakano I, Ozawa K. Adeno-associated virus vectors for gene transfer to the brain. *Methods*. 2002;28:237–247.
13. Kay JM, Keane PM, Suyama KL, Gauthier D. Angiotensin converting enzyme activity and evolution of pulmonary vascular disease in rats with monocrotaline pulmonary hypertension. *Thorax*. 1982;37:88–96.
14. Christman BW, McPherson CD, Newman JH, King GA, Bernard GR, Groves BM, Loyd JE. An imbalance between the excretion of thromboxane and prostacyclin metabolites in pulmonary hypertension. *N Engl J Med*. 1992;327:70–75.
15. Tuder RM, Cool CD, Geraci MW, Wang J, Abman SH, Wright L, Badesch D, Voelkel NF. Prostacyclin synthase expression is decreased in lungs from patients with severe pulmonary hypertension. *Am J Respir Crit Care Med*. 1999;159:1925–1932.
16. Miyata A, Hara S, Yokoyama C, Inoue H, Ullrich V, Tanabe T. Molecular cloning and expression of human prostacyclin synthase. *Biochem Biophys Res Commun*. 1994;200:1728–1734.
17. High K. AAV-mediated gene transfer for hemophilia. *Genet Med*. 2002; 4:56S–61S.
18. Phillips PG, Long L, Wilkins MR, Morrell NW. cAMP phosphodiesterase inhibitors potentiate effects of prostacyclin analogs in hypoxic pulmonary vascular remodeling. *Am J Physiol Lung Cell Mol Physiol*. 2005;288: L103–L115.
19. Ali FY, Egan K, FitzGerald GA, Desvergne B, Wahli W, Bishop-Bailey D, Warner TD, Mitchell JA. Role of prostacyclin versus peroxisome proliferator-activated receptor beta receptors in prostacyclin sensing by lung fibroblasts. *Am J Respir Cell Mol Biol*. 2006;34:242–246.
20. Ameshima S, Golpon H, Cool CD, Chan D, Vandivier RW, Gardai SJ, Wick M, Nemenoff RA, Geraci MW, Voelkel NF. Peroxisome proliferator-activated receptor gamma (PPARgamma) expression is decreased in pulmonary hypertension and affects endothelial cell growth. *Circ Res*. 2003;92:1162–1169.
21. Sitbon O, Humbert M, Nunes H, Parent F, Garcia G, Herve P, Rainisio M, Simonneau G. Long-term intravenous epoprostenol infusion in primary pulmonary hypertension: prognostic factors and survival. *J Am Coll Cardiol*. 2002;40:780–788.
22. Nathwani AC, Gray JT, McIntosh J, Ng CY, Zhou J, Spence Y, Cochrane M, Gray E, Tuddenham EG, Davidoff AM. Safe and efficient transduction of the liver after peripheral vein infusion of self-complementary AAV vector results in stable therapeutic expression of human FIX in nonhuman primates. *Blood*. 2007;109:1414–1421.

EXPERIMENTAL and MOLECULAR MEDICINE, Vol. 39, No. 2, 170-175, April 2007

Promoter effects of adeno-associated viral vector for transgene expression in the cochlea *in vivo*

Yuhe Liu[1,3], Takashi Okada[2], Tatsuya Nomoto[2], Xiaomei Ke[1], Akihiro Kume[2], Keiya Ozawa[2] and Shuifang Xiao[1]

[1]Department of Otolaryngology
Head and Neck Surgery, Peking University First Hospital
Beijing 100034, China
[2]Division of Genetic Therapeutics
Center for Molecular Medicine
Jichi Medical School
Tochigi 329-0498, Japan
[3]Corresponding author: Tel, 86-10-63078547;
Fax, 86-10-66173427; E-mail, liuyuhe@xinhuanet.com

Accepted 6 February 2007

Abbreviations: AAV, adeno-associated virus; CAG, cytomegalovirus IE enhancer and chicken β-actin promoter; CMV, cytomegalovirus promoter; EF-1α, elongation factor 1 alpha promoter; EGFP, enhanced green fluorescent protein; ITRs, inverted terminal repeats; Myo, myosin 7A promoter; NSE, neuron-specific enolase promoter; RSV, Rous sarcoma virus promoter; WPRE, woodchuck hepatitis; virus posttranscriptional regulatory element

Abstract

The aims of this study were to evaluate the expression of enhanced green fluorescent protein (EGFP) driven by 6 different promoters, including cytomegalovirus IE enhancer and chicken β–actin promoter (CAG), cytomegalovirus promoter (CMV), neuron-specific enolase promoter (NSE), myosin 7A promoter (Myo), elongation factor 1α promoter (EF-1α), and Rous sarcoma virus promoter (RSV), and assess the dose response of CAG promoter to transgene expression in the cochlea. Serotype 1 adeno-associated virus (AAV1) vectors with various constructs were transduced into the cochleae, and the level of EGFP expression was examined. We found the highest EGFP expression in the inner hair cells and other cochlear cells when CAG promoter was used. The CMV and NSE promoter drove the higher EGFP expression, but only a marginal activity was observed in EF-1α promoter driven constructs. RSV promoter failed to drive the EGFP expression. Myo promoter driven EGFP was exclusively expressed in the inner hair cells of the cochlea. When driven by CAG promoter, reporter gene expression was detected in inner hair cells at a dose as low as 3×10^7 genome copies, and continued to increase in a dose-dependent manner. Our data showed that individual promoter has different ability to drive reporter gene expression in the cochlear cells. Our results might provide important information with regard to the role of promoters in regulating transgene expression and for the proper design of vectors for gene expression and gene therapy.

Keywords: cochlea; dependovirus; gene therapy; gene transfer techniques; green fluorescent proteins; promoter regions

Introduction

Gene transfer is a promising tool to study the physiology of the cochlea and cochlear cells. The feasibility of gene therapy in the cochlea has been established (Dazert *et al.*, 2001; Kawamoto *et al.*, 2001; Liu *et al.*, 2005), still, there is a controversy about the transduction of the hair cells or spiral ganglion cell, even when the same vehicle is employed as vectors, such as adenovirus and adeno-associated virus (AAV) (Luebke *et al.*, 2001; Li *et al.*, 2002; Yamasoba *et al.*, 2002; Liu *et al.*, 2005). The previous studies support the hypothesis that this discrepancy may be caused by the differences in delivery methods or driven promoters. It has been shown that individual promoter has distinct ability to express reporter genes in different cell types (Chung *et al.*, 2002; Nomoto *et al.*, 2003; Shevtsova *et al.*, 2005). Tissue or cell specific promoters are capable of restricting gene expression in desirable cells and facilitating persistent or regulated transgene expression (Liu *et al.*, 2004). The cytomegalovirus IE enhancer and chicken β-actin promoter (CAG) drives high level of transgene expression and is one of the most commonly used promoters for gene transfer (Xu *et al.*, 2001). The myosin 7A promoter (Myo) was shown to be the specific promoter of hair cells in the cochlea (Boeda *et al.*, 2001). We have previously demonstrated that, with AAV1 vectors, the CAG promoter can drive transgene expression in the cochlea cells at a highly functional level (Liu *et al.*, 2005). In the present study, we systematically evaluated the promoters CAG, Myo, cytomegalovirus

promoter (CMV), elongation factor 1 alpha promoter (EF-1α), neuron-specific enolase promoter (NSE), and rous sarcoma virus promoter (RSV) for their abilities in gene transfers to the cochlear cells using *in vivo* assays. We also examined the dose-response relationship for CAG promoter over a broad range in the cochlea.

Materials and Methods

Construction and preparation of the proviral plasmids

The AAV1 vector proviral plasmid, pAAV2-*LacZ*, harbors an *Escherichia coli* β-galactosidase expression cassette with the CMV promoter, human growth hormone first intron, and SV40 early polyadenylation sequence; flanked by inverted terminal repeats (ITRs) (Okada *et al.*, 2002). The proviral plasmid pAAV2-CAG-EGFP-WPRE (pAAV2-CAG) consists of enhanced green fluorescent protein (EGFP) gene under the control of the CAG promoter and Woodchuck hepatitis virus posttranscriptional regulatory element (WPRE) and is flanked by ITRs (Liu *et al.*, 2005). *Age*I restriction site was created on 5' end of Myo promoter (Boeda *et al.*, 2001) from C2C12 cell line genomic DNA when subcloned into pCRII-TOPO by PCR (forward primer: 5'-ATGTCGACCT-TGGGCAACCTCTAGACG-3'; reverse primer: 5'-ATC-CGCGGCTTCTACGTCTGCACAC-3'). *Spe*I-*Age*I fragment containing the Myo promoter was subcloned into pAAV2-CAG to obtain pAAV2-Myo-EGFP-WPRE (pAAV2-Myo). PAAV2-CMV-EGFP-WPRE (pAAV2-CMV), pAAV2-EF1α-EGFP-WPRE (pAAV2-EF1α), pAAV2-NSE-EGFP-WPRE (pAAV2-NSE), and pAAV2-RSV-EGFP-WPRE (pAAV2-RSV) were constructed as previously described (Ogasawara *et al.*, 1998; Nomoto *et al.*, 2003; Mochizuki *et al.*, 2004). A schematic illustration of the AAV1 vectors is shown in Figure 1. AAV1-helper plasmid harbors Rep and Cap. Adenovirus helper plasmid pAdeno5 identical to pVAE2AE4-5 encodes the entire E2A and E4 regions, and VA RNA I and II genes (Matsushita *et al.*, 1998). Plasmids were purified with the QIAGEN plasmid purification Kits (QIAGEN K.K., Tokyo, Japan).

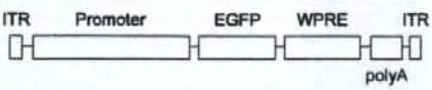

Figure1. Schematic representations of viral vectors constructed. AAV1 vectors were constructed using different promoters to drive reporter gene EGFP and the SV40 polyadenylation sequences (polyA). The promoters in the study include CAG, CMV, NSE, Myo, EF-1α and RSV. The Woodchuck hepatitis virus posttranscriptional regulatory element (WPRE) was inserted 3' of the EGFP cassette in the vectors. ITR, inverted terminal repeats.

Recombinant AAV1 vectors production

Vectors were produced with the AAV1 packaging plasmids pAAV1RepCap and the AAV1 proviral plasmid pAAV2-CAG, pAAV2-Myo, pAAV2-CMV, pAAV2-EF1α, pAAV2-NSE, or pAAV2-RSV. Six kinds of AAV1 vectors were produced using three-plasmid transfection adenovirus-free protocol (Liu *et al.*, 2005). Recombinant AAV1 was harvested at 72 h after transfection by three cycles of freeze/thawing. The crude viral lysate was then purified twice on a cesium chloride (CsCl) two-tier centrifugation gradient as previously described (Okada *et al.*, 2002). The viral stock was titrated by the quantitative real-time PCR of DNase-treated stocks with plasmid standards (Veldwijk *et al.*, 2002). Thus, AAV1 vectors of AAV1-CAG-EGFP-WPRE (AAV1-CAG), AAV1-Myo-EGFP-WPRE (AAV1-Myo), AAV1-CMV-EGFP-WPRE (AAV1-CMV), AAV1-EF1α-EGFP-WPRE (AAV1-EF1α), AAV1-NSE-EGFP-WPRE (AAV1-NSE), and AAV1-RSV-EGFP-WPRE (AAV1-RSV) were constructed. The titers of AAV1 vectors were from 6×10^{12} to 8×10^{13} genome copies (g.c.). For dose-response relationship experiment, vector stocks were serially diluted with artificial perilymph (AP: 145 mM NaCl, 2.7 mM KCl, 2 mM $MgSO_4$, 1.2 mM $CaCl_2$, 5 mM HEPES).

Evaluation of the *in vitro* activity of recombinant AAV1 vectors

To examine the functions of individual promoters, HEK 293 cells were cultured for 36 h, and then transfected with various AAV1 vectors separately (1×10^4 g.c./cell). *Myosin 7A* gene is transcribed in several epithelial cell types that possess microvilli, i.e. renal epithelial cell. Since HEK 293 cell line has been originated from human embryonic kidney epithelial cell, the Myo promoter activity can be assessed in this particular cell line. Forty-eight h after transduction, the cells were recorded for EGFP expression using OLYMPUS IX70 (Olympus corporation, Tokyo, Japan) fluorescence microscope. Cells with green fluorescence were considered "positive" for transgene expression.

Surgical procedures and cochlear perfusions

All animal studies were approved by the ethics committee of Jichi Medical School in Japan and Peking University First Hospital in China. They were performed following the animal research guidelines at Jichi Medical School and Peking University First

Hospital. Seventy female C57BL/6J mice (4 weeks old, CLEA Japan, Tokyo, Japan) and 30 male Sprague-Dawley rats (5 weeks old, CLEA Japan, Tokyo, Japan) with normal Preyer's reflexes were included in this study. Surgical procedures and cochlear perfusion of the animals were performed as previously described (Liu *et al.*, 2005). In the testing groups, 5 μl of AAV1 vectors solution was microinjected into the unilateral cochlea. Five mice received control cochlear perfusions with artificial perilymph only. Each AAV1 vector was injected into 5 animals with 3×10^{10} g.c./cochlea. Injected dose of AAV1-CAG vector into 5 mice was varied from 3×10^{10} to 3×10^{7} g.c./cochlea for dose response study.

Histological study

The capability of the transgene expression in the cochlear cells for various AAV1 vectors was determined by visualizing EGFP levels. The animals were sacrificed 2 weeks after injection, and the cochleae were harvested and the stapes footplates were removed. After fixing and decalcifying, the cochleae were made by cryosection (10 μm). The EGFP expression was detected under OLYMPUS IX70 fluorescence microscope using a standard fluoresce in isothiocyanate (FITC) filter set and a Studio Lite software (Olympus corporation, Tokyo, Japan). Level of expression was graded by fluorescent intensity.

Results

Evaluation of activity of all promoters *in vitro*

The EGFP expression in the HEK 293 cell was detected with any of the AAV1 vectors, indicating that all promoters were functional. However, their expression levels were different (Figure 2). Robust EGFP expression with CAG promoter was shown in the HEK 293 cell, followed by CMV, NSE, EF-1α and RSV. Myo promoter was just weak in 293 cells.

EGFP expression profile within the cochlea under different promoter

The pattern of EGFP expression in the cochlear cells was quite similar in both mice and rat for each promoter. Distribution of AAV1 vector-mediated EGFP expression was examined throughout the cochlea for all promoters tested (Table 1). With CAG promoter, a robust EGFP expression was identified in the various cochlear cells, including the inner hair cells, spiral ganglion cells, inner sulcus cells, Hensen's cells and mesenchymal cells (Figure 3B). A

Figure 2. EGFP expression in the HEK293 cell transduced with AAV1 vectors harboring distinct promoters. Robust EGFP expression with CAG promoter was shown, EGFP expression with CMV is similar to that with CAG, and EGFP expression with NSE to with RSV and EF-1α. Myo promoter was just weak in 293 cells.

Table 1. Transgene expression with distinct promoter in the cochlear cells

Promoter	Inner hair cells	Outer hair cells	Spiral ganglion cells	Stria vascularis cells	Spiral ligament cells	Reissner's membrane	Inner sulcus cells	Claudius' cells	Mesenchymal cells
CAG	+	-	+	-	+	+	+	-	+
CMV	+	-	+	-	+	+	+	-	+
NSE	-	-	+	-	+	+	-	-	+
EF-1α	-	-	+	-	+	-	-	-	+
Myo	+	-	-	-	-	-	-	-	-
RSV	-	-	-	-	-	-	-	-	-

+ means EGFP expression in the cells, while - means no fluorescence in the cells.

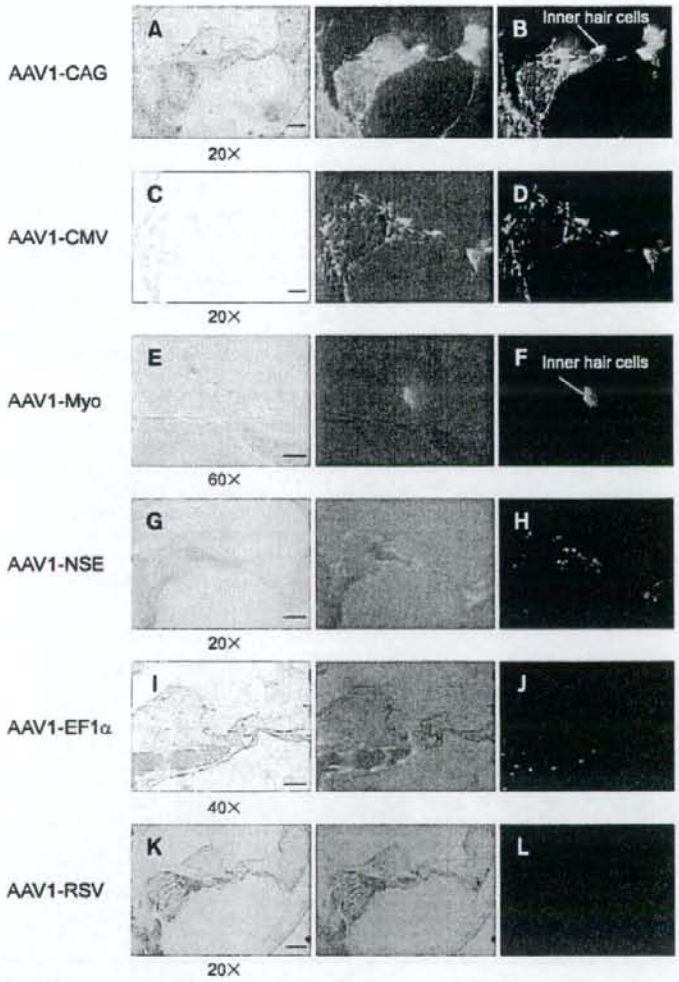

Figure 3. Transduction of cochlear radical cryosection with AAV1 vectors harboring distinct promoters showing EGFP expression in the cochlear various cells. Light photomicrograph of cochlear cryosection is shown in (A,C,E,G,I,K). The fluorescence photomicrograph (green fluorescence from transgene) of the cryosection is shown in (B,D,F,H,J,L). Scale bar, 20×: 50; 40×: 25; 60×: 25 μm separately.

similar transgene expression pattern (Figure 3D) was also observed when AAV1-CMV vector was used. In contrast, the EGFP expression under NSE and EF- 1α promoters was present in all kinds but the inner hair cells of cochlear cells (Figure 3H and J). As reported previously (Boeda *et al.*, 2001), Myo promoter driven EGFP was exclusively expressed in the inner hair cells of cochlea (Figure 3F), while EGFP expression in the cochlear cells was rarely observed with the RSV promoter (Figure 3L). Consistent with the previous findings (Liu *et al.*, 2005), no EGFP expression was detected in the outer hair cells, supporting pillar cells, or the stria vascularis cells with all tested promoters. The level of EGFP expression in the cochlear cells was highest with CAG promoter, followed by CMV promoter. NSE promoter only drove weak expression of EGFP, while EF-1α promoter displayed the least activity.

Our results indicate that, among these promoters, CAG promoter was the most efficient in transducing the cochlear cells.

Dose-response relationship for AAV1-CAG vector

Within the dose-effect groups with AAV1-CAG, a significant effect of dosage on the number of EGFP-expressing cochlear cells was found by one-way ANOVA ($P < 0.001$). CAG promoter driven EGFP expression in inner hair cells was detected at a dose as low as 3×10^7 genome copies, with expression increasing in a dose-dependent manner.

Discussion

The various factors affecting the transcription of a transgene includes the promoter containing 5'flanking region, 3'UTR, enhancer, suppressor, insulator sequences and the type and activity of transcription factors available in the transfected cells. This study showed that all 6 promoters, including viral, mammalian cells promoters, were capable of driving EGFP expression in HEK 293 cells, suggesting that the HEK 293 cell possesses all essential transcription factors for recognizing the diverse promoter sequences applied in this study. The CAG promoter appeared to be more efficient than other promoters based on the following observations: (1) more cells transduced in an equal dose comparison; (2) greater spreads of EGFP-expressing cell groups; and (3) CAG promoter-driven expression in more cell types, especially the inner hair cells, which were rarely found with other promoters except for CMV promoter. These results extend our knowledge about the promoter-related characteristics of AAV1-mediated gene transfer in the cochlea.

Interestingly, our data demonstrate that, in comparison with NSE, EF-1α and RSV promoters, CAG, CMV and hair cells specific promoter-Myo can drive EGFP expression in the inner hair cells. Even though certain promoters, such as EF-1α and RSV promoters, showed robust activity in many tissues, their activities are limited in the cochlear cells. Nowadays, it still has not been known why NSE, EF-1α and RSV promoters are inactive in the inner hair cells. One likely explanation is that inner hair cells may not express some transcription factors, which were necessary for these promoters to be actived. On the other hand, the inner hair cells may have all necessary components for the full transcriptional activity of the CAG, CMV or Myo promoters. Another possibility is transcriptional shutdown or promoter silencing in the inner hair cells. These phenomena have been observed previously in different organs such as the liver, lungs, and muscles (Hartikka *et al.*, 1996; Chen *et al.*, 2001; Gill *et al.*, 2001). Besides the known mechanisms for promoter silencing, such as DNA methylation, it has been demonstrated that the inclusion of EBN1 and OriP sequences into vector constructs may delay the process of promoter silencing (Al-Dosari *et al.*, 2006). Those elements also have been known to play an important role during viral infection in retention, replication, nuclear localization, binding to the nuclear matrix of the target cell, and tran-scriptional up-regulation (Cui *et al.*, 2001). Nevertheless, the mechanism of promoter inactivation remains to be poorly understood. The development of the vectors, which was capable of expressing high levels of transgene products, remains as an occasional finding. A thorough investigation on the mechanisms underlying episomal gene expression would be important for successful development of gene therapy.

Dose-dependent response for AAV gene transfer in other tissue has been previously reported (Klein *et al.*, 2002), and the wide range of doses has established minimal doses for transgene expression (10^7 particles). There is a shift toward lower potency for bicistronic vectors. The present study determined the dose dependency and minimum effective doses for AAV1 gene transfer using CAG promoter for the cochlear cells.

The direct measurement of transgene expression level in individual cells of cochlea *in vivo* is an important evaluation for cochlear gene therapy. Nevertheless, quantifying the number of cells transduced remains an important additional issue and a combination of protein expression and cell transduction efficiency may permit us to estimate the amount of gene product per cell under appropriate conditions. The gene transduction of the cochlear inner hair cells requires efficient promoter systems, which ensure potent and stable expression of exogenous genes. In this study, we demonstrated that the CAG and CMV promoters showed stable and efficient activity in the cochlear cells, the Myo promoter was specific for gene transfer in the inner hair cells. The stable and efficient promoter activities might be necessary for cochlear gene therapy strategies. From the data obtained by this study, it might be able to extend our knowledge both in the basic and clinical gene research fields.

Acknowledgement

This study was supported in part by Research Grants from the Ministry of Education, Culture, Sports, Science and Technology, the Ministry of Health, Labor and Welfare, and the Vehicle Racing Commemorative Foundation.

References

Al-Dosari M, Zhang G, Knapp JE, Liu D. Evaluation of viral and mammalian promoters for driving transgene expression in mouse liver. Biochem Biophys Res Commun 2006;339:673-8

Boeda B, Weil D, Petit C. A specific promoter of the sensory cells of the inner ear defined by transgenesis. Hum Mol Genet 2001;10:1581-9

Chen ZY, Yant SR, He CY, Meuse L, Shen S, Kay MA. Linear DNAs concatemerize *in vivo* and result in sustained transgene expression in mouse liver. Mol Ther 2001;3:403-10

Chung S, Andersson T, Sonntag KC, Bjorklund L, Isacson O, Kim KS. Analysis of different promoter systems for efficient transgene expression in mouse embryonic stem cell lines. Stem Cells 2002;20:139-45

Cui FD, Kishida T, Ohashi S, Asada H, Yasutomi K, Satoh E, Kubo T, Fushiki S, Imanishi J, Mazda O. Highly efficient gene transfer into murine liver achieved by intravenous administration of naked Epstein-Barr virus (EBV)-based plasmid vectors. Gene Ther 2001;8:1508-13

Dazert S, Aletsee C, Brors D, Gravel C, Sendtner M, Ryan A. *In vivo* adenoviral transduction of the neonatal rat cochlea and middle ear. Hear Res 2001;151:30-40

Gill DR, Smyth SE, Goddard CA, Pringle IA, Higgins CF, Colledge WH, Hyde SC. Increased persistence of lung gene expression using plasmids containing the ubiquitin C or elongation factor 1alpha promoter. Gene Ther 2001;8:1539-46

Hartikka J, Sawdey M, Cornefert-Jensen F, Margalith M, Barnhart K, Nolasco M, Vahlsing HL, Meek J, Marquet M, Hobart P, Norman J, Manthorpe M. An improved plasmid DNA expression vector for direct injection into skeletal muscle. Hum Gene Ther 1996;7:1205-17

Kawamoto K, Oh SH, Kanzaki S, Brown N, Raphael Y. The functional and structural outcome of inner ear gene transfer via the vestibular and cochlear fluids in mice. Mol Ther 2001;4:575-85

Klein RL, Hamby ME, Gong Y, Hirko AC, Wang S, Hughes JA, King MA, Meyer EM. Dose and promoter effects of adeno-associated viral vector for green fluorescent protein expression in the rat brain. Exp Neurol 2002;176: 66-74

Li Duan M, Bordet T, Mezzina M, Kahn A, Ulfendahl M. Adenoviral and adeno-associated viral vector mediated gene transfer in the guinea pig cochlea. Neuroreport 2002;13: 1295-9

Liu BH, Wang X, Ma YX, Wang S. CMV enhancer/human PDGF-beta promoter for neuron-specific transgene expression. Gene Ther 2004;11:52-60

Liu Y, Okada T, Sheykholeslami K, Shimazaki K, Nomoto T, Muramatsu SI, Kanazawa T, Takeuchi K, Ajalli R, Mizukami H, Kume A, Ichimura K, Ozawa K. Specific and efficient transduction of cochlear inner hair cells with recombinant adeno-associated virus type 3 vector. Mol Ther 2005;12:725-733

Luebke AE, Foster PK, Muller CD, Peel AL. Cochlear function and transgene expression in the guinea pig cochlea, using adenovirus- and adeno-associated virus-directed gene transfer. Hum Gene Ther 2001;12:773-81

Matsushita T, Elliger S, Elliger C, Podsakoff G, Villarreal L, Kurtzman GJ, Iwaki Y, Colosi P. Adeno-associated virus vectors can be efficiently produced without helper virus. Gene Ther 1998;5:938-45

Mochizuki S, Mizukami H, Kume A, Muramatsu S, Takeuchi K, Matsushita T, Okada T, Kobayashi E, Hoshika A, Ozawa K. Adeno-associated virus (AAV) vector-mediated liver- and muscle-directed transgene expression using various kinds of promoters and serotypes. Gene ther Mol Biol 2004;8:9-18

Nomoto T, Okada T, Shimazaki K, Mizukami H, Matsushita T, Hanazono Y, Kume A, Katsura K, Katayama Y, Ozawa K. Distinct patterns of gene transfer to gerbil hippocampus with recombinant adeno-associated virus type 2 and 5. Neurosci Lett 2003;340:153-7

Ogasawara Y, Urabe M, Ozawa K. The use of heterologous promoters for adeno-associated virus (AAV) protein expression in AAV vector production. Microbiol Immunol 1998;42:177-85

Okada T, Nomoto T, Shimazaki K, Lijun W, Lu Y, Matsushita T, Mizukami H, Urabe M, Hanazono Y, Kume A, Muramatsu S, Nakano I, Ozawa K. Adeno-associated virus vectors for gene transfer to the brain. Methods 2002;28:237-47

Shevtsova Z, Malik JM, Michel U, Bahr M, Kugler S. Promoters and serotypes: targeting of adeno-associated virus vectors for gene transfer in the rat central nervous system *in vitro* and *in vivo*. Exp Physiol 2005;90:53-9

Veldwijk MR, Topaly J, Laufs S, Hengge UR, Wenz F, Zeller WJ, Fruehauf S. Development and optimization of a real-time quantitative PCR-based method for the titration of AAV-2 vector stocks. Mol Ther 2002;6:272-8

Xu L, Daly T, Gao C, Flotte TR, Song S, Byrne BJ, Sands MS, Parker Ponder K. CMV-beta-actin promoter directs higher expression from an adeno-associated viral vector in the liver than the cytomegalovirus or elongation factor 1 alpha promoter and results in therapeutic levels of human factor X in mice. Hum Gene Ther 2001;12:563-73

Yamasoba T, Suzuki M, Kondo K. Transgene expression in mature guinea pig cochlear cells *in vitro*. Neurosci Lett 2002;335:13-6

THE JOURNAL OF GENE MEDICINE
J Gene Med 2008; **10**: 368–374.
Published online 21 January 2008 in Wiley InterScience (www.interscience.wiley.com) **DOI:** 10.1002/jgm.1166

RESEARCH ARTICLE

Adeno-associated virus vector-mediated systemic interleukin-10 expression ameliorates hypertensive organ damage in Dahl salt-sensitive rats

Mutsuko Nonaka-Sarukawa[1,2]
Takashi Okada[1]
Takayuki Ito[1,2]*
Keiji Yamamoto[2]
Toru Yoshioka[3]
Tatsuya Nomoto[1]
Yukihiro Hojo[2]
Masahisa Shimpo[2]
Masashi Urabe[1]
Hiroaki Mizukami[1]
Akihiro Kume[1]
Uichi Ikeda[3]
Kazuyuki Shimada[2]
Keiya Ozawa[1]*

[1]*Division of Genetic Therapeutics, Jichi Medical University, Japan*

[2]*Division of Cardiovascular Medicine, Jichi Medical University, Japan*

[3]*Department of Organ Regeneration, Shinshu University Graduate School of Medicine, Japan*

*Correspondence to: Takayuki Ito and Keiya Ozawa, Division of Genetic Therapeutics, Centre for Molecular Medicine, Jichi Medical University, 3311-1 Yakushiji, Shimotsuke-shi, Tochigi 329-0498, Japan.
E-mail: titou@jichi.ac.jp and kozawa@jichi.ac.jp

Received: 5 October 2007
Revised: 26 November 2007
Accepted: 11 December 2007

Abstract

Background Inflammation plays an important role in the pathogenesis of hypertension and hypertensive organ damage. Interleukin (IL)-10, a pleiotropic anti-inflammatory cytokine, exerts vasculoprotective effects in many animal models. In the present study, we examined the preventive effects of adeno-associated virus (AAV) vector-mediated sustained IL-10 expression against hypertensive heart disease and renal dysfunction in Dahl salt-sensitive rats.

Methods We injected the rats intramuscularly with an AAV type 1-based vector encoding rat IL-10 or enhanced green fluorescent protein (EGFP) at 5 weeks of age; subsequently, the rats were fed a high-sodium diet from 6 weeks of age.

Results Sustained IL-10 expression significantly improved survival rate of Dahl salt-sensitive rats compared with EGFP expression (62.5% versus 0%, $p < 0.001$); it also caused 26.0% reduction in systolic blood pressure at 15 weeks ($p < 0.0001$). Echocardiography exhibited a 22.0% reduction in hypertrophy ($p < 0.0001$) and a 26.3% improvement in fractional shortening ($p < 0.0001$) of the rat left ventricle in the IL-10 group compared to the EGFP group. IL-10 expression also caused a 21.7% decrease in the heart weight/body weight index and cardiac atrial natriuretic peptide levels. Histopathological studies revealed that IL-10 decreased inflammatory cell infiltration, fibrosis, and transforming growth factor-β_1 levels in the failing heart. Furthermore, IL-10 expression significantly reduced urine protein excretion with increased glomerular filtration rates.

Conclusions This is the first study to demonstrate that the anti-inflammatory cytokine IL-10 has a significant anti-hypertensive effect. AAV vector-mediated IL-10 expression potentially prevents the progression of refractory hypertension and hypertensive organ damage in humans. Copyright © 2008 John Wiley & Sons, Ltd.

Keywords AAV vector; gene therapy; hypertension; inflammation; interleukin-10

Introduction

Inflammation plays an important role in the pathogenesis of hypertension and hypertensive organ damage. Congestive heart failure (CHF) is a crucial life-threatening sequalae of hypertensive organ damage, and

its severity is closely related with the serum tumor necrosis factor (TNF) levels [1,2]. Recent studies have demonstrated the marked anti-hypertensive and renoprotective effects of an immunosuppressant *in vivo* [3,4]. Although these observations suggest a therapeutic potential of anti-inflammatory molecules, anti-TNF antibody treatments (e.g. infliximab and etanercept) have failed to improve the survival of CHF patients partly because of their cytokine-inducing effects and cytotoxicity [5,6].

Interleukin (IL)-10 is a pleiotropic cytokine produced by monocytes/macrophages and type 2 helper T cells. It regulates inflammatory and immune reactions by inhibiting macrophage activation, T-cell proliferation, and the production of proinflammatory cytokines such as TNF-α [7]. IL-10 also enhances endothelial nitric oxide synthase expression [8] and inhibits vascular smooth muscle cell proliferation [9,10]. Previous studies have demonstrated the therapeutic effects of IL-10 on CHF models resulting from acute viral or autoimmune myocarditis [11,12]. However, no studies have examined the effects of IL-10 on chronic CHF resulting from hypertensive heart disease that occurs far more frequently than acute myocarditis. In the present study, we examined the effects of IL-10 using Dahl salt-sensitive (DS) rats that present with severe hypertension and chronic CHF when fed a salt-rich diet [13].

We employed an adeno-associated virus (AAV) type 1-based vector in order to sustain serum levels of IL-10 because it has a short biological half-life. AAV vectors permit long-term transgene expression with minimal inflammatory and immune responses [14]. If the intramuscular injection of the AAV serotype 1 vector carrying the IL-10 gene (AAV1-IL-10) produces sufficient amount of IL-10 in skeletal myocytes, then IL-10 should be secreted into the systemic circulation [10]. We examined the preventive effects of IL-10 on chronic CHF progression in DS rats, focusing on its effects on survival, hypertension, pathological cardiac remodelling and renal function.

Materials and methods

AAV vector production

Rat IL-10 was cloned from rat splenocyte cDNA by the polymerase chain reaction (PCR) using the primers: 5′-GCACGAGAGCCACAACGCA-3′ (upstream) and 5′-GATTTGAGTACGATCCATTTATTCAAAACGAGGAT-3′ (downstream) [10]. To achieve efficient transduction of the skeletal muscles, we developed a recombinant AAV type 1-based vector encoding rat IL-10 (AAV1-IL-10) or enhanced green fluorescence protein (EGFP, AAV1-EGFP) controlled by the modified chicken β-actin promoter with the cytomegalovirus immediate–early enhancer and by the woodchuck hepatitis virus post-transcriptional regulatory element [pBS II SK (+) WPRE-B11, provided by Dr Thomas Hope, University of Illinois, Chicago, IL, USA]. The AAV vectors were prepared by the previously described three-plasmid transfection adenovirus-free protocol modified by the use of the active gassing system [15,16]. Briefly, 60% confluent human embryonic kidney 293 cells were co-transfected with the proviral transgene plasmid, the AAV-1 chimeric helper plasmid p1RepCap (provided by Dr James M. Wilson, University of Pennsylvania, Philadelphia, PA, USA), and the adenoviral helper plasmid pAdeno (provided by Avigen, Inc., Alamada, CA, USA). The crude viral lysate was purified by two rounds of two-tier CsCl centrifugation [14]. The viral stock titer was determined by dot blot hybridization with plasmid standards.

Animal experiment protocols

All animal studies were performed in accordance with the guidelines issued by the committee on animal research and approved by the ethics committee of Jichi Medical University. For histopathological and physiological studies (Protocol 1; Figure 1), we divided the male DS rats (Japan SLC, Shizuoka, Japan) into the following three groups:

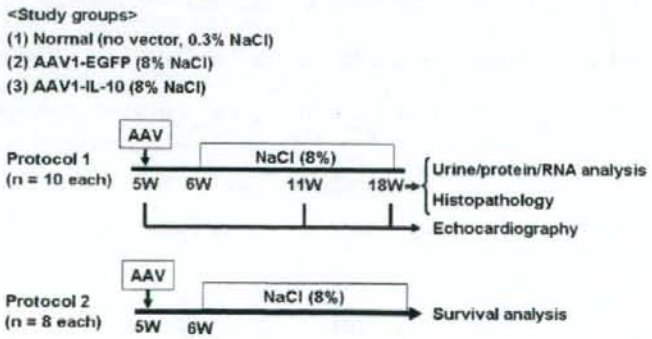

Figure 1. Study protocols. The male DS rats were divided into the three groups: (1) normal group, (2) EGFP group, and (3) IL-10 group. The rats without normal group were injected with AAV1 vectors at 5 weeks of age. The rats in the normal group were fed a low-sodium diet (containing 0.3% NaCl), whereas those in the EGFP or IL-10 group were fed a high-sodium diet (containing 8% NaCl) from 6 weeks of age

IL-10, EGFP and normal ($n = 10$, respectively). AAV1-IL-10 or AAV1-EGFP [1×10^{12} genome copies (g.c.)/body] was injected bilaterally into the anterior tibial muscles of the 5-week-old rats in the IL-10 or EGFP groups, respectively. From 6 weeks onwards, these rats were fed a high-sodium diet (containing 8% NaCl). DS rats in the normal group were fed a low-sodium diet (containing 0.3% NaCl). Systolic blood pressure (SBP) was measured every 2 weeks by the tail-cuff method using a manometer tachometer (MK-1030; Muromachi Kikai Co., Ltd, Tokyo, Japan). During the acclimatization period (3–5 weeks), training for blood pressure measurements was performed three times a week. The mean of the three measurements following a 10-min rest at 37 °C was used in the calculations. Blood was collected from the tail vein at 5,11 and 18 weeks; the sera and plasma were stored at −80 °C. At 18 weeks, the rats were sacrificed by administering an overdose of isoflurane, and their hearts and lungs were harvested and weighed. The tissues were immediately frozen in liquid nitrogen and stored at −80 °C to obtain proteins and RNA for the subsequent analysis. For survival analysis (Protocol 2; Figure 1), the rats were randomly divided into three groups ($n = 8$ each). Those in the IL-10 or EGFP group were injected at 5 weeks of age with the AAV1-IL-10 or AAV1-EGFP (1×10^{11} g.c./body), respectively, and this was followed by a high-sodium diet from 6 weeks of age. By contrast, those in the normal group were fed a low-sodium diet.

Echocardiography

Transthoracic two-dimensional echocardiography was performed at 5, 11 and 18 weeks of age using a 13- MHz transducer (ProSound SSD-α5; Aloka Co., Ltd, Tokyo, Japan). The internal diameter in end-diastole or end-systole of the left ventricle (LVDd or LVDs, respectively) or the posterior wall thickness (PWT) of the left ventricle (LV) in end-diastole was measured by M-mode tracing at the papillary muscle level. The relative wall thickness (RWT) or the percentage fractional shortening (%FS) of LV was calculated according to the formula: RWT = $2 \times$ PWT/LVDd, %FS = (LVDd − LVDs)/LVDd $\times$ 100 (%).

Cytokine measurements

At 18 weeks, protein samples were prepared by homogenizing the frozen heart tissues in a lysis buffer [10 mmol/l Tris-HCl (pH 8.0), 0.2% NP40, 1 mmol/l ethylenediaminetetraacetic acid] containing the protease inhibitor cocktail Complete Mini (Roche Diagnostics, Mannheim, Germany). After centrifugation of the homogenates or serum samples, the supernatants were used for measurement. The serum IL-10 and the tissue transforming growth factor (TGF)-β_1 concentrations were measured by enzyme-linked immunosorbent assay (ELISA) (Amersham PharmaciaBiotech, Bucks, UK; BioSource International, Inc., Camarillo, CA, USA; R&D Systems Inc., Minneapolis, MN, USA). The tissue cytokine levels were standardized using the total protein concentrations estimated by the BCA Protein Assay Kit (Pierce, Rockford, IL, USA).

Quantitative reverse transcriptase (RT)-PCR

At 18 weeks, total RNA was extracted from the heart by using RNAzol B (Tel-Test, Inc., Friendswood, TX, USA) and reverse-transcribed into double-stranded cDNA by using the Superscript Preamplification System (Invitrogen, Carlsbad, CA, USA) with the T7-dT primer (5′-GGCCAGTGAATTGTAATACGACTCACTATAGGGA-GGCGGTTTTTTTTTTTTTTTTTTTTTTTT-3′). To estimate the atrial natriuretic protein (ANP) mRNA levels, quantitative PCR analysis was conducted using the ABI Prism 7900 Sequence Detection System (Applied Biosystems, Foster City, CA, USA). The GAPDH mRNA was quantified for normalization. The oligonucleotide primers used were: for GADPH, 5′-CAGCAATGCAT CCTGCAC-3′ (upstream) and 5′-GAGTTGCTGTTGAAGTCACAGG-3′ (downstream) [17]; for ANP, 5′-GGTAGGATTGACAGGATTGGAGCC-3′ (upstream) and 5′-ACATCGATCGTGATAGATGAAGAC-3′ (downstream) [18]. Quantitative values were obtained from the threshold cycle (C_t) number that indicates exponential amplification of a PCR product.

Histopathology

At 18 weeks of age, the anesthetized rats were perfused with 50 ml of saline, followed by 100 ml of cold 4% paraformaldehyde in 0.1 mol/l phosphate buffer (pH 7.4). The hearts were fixed in the same fixative and finally embedded in paraffin. For evaluation of light microscopic findings, we stained sections (3 μm thick) with hematoxylin and eosin (H&E) or the Azan–Mallory stain using the standard methods.

Statistical analysis

The data were assessed using the StatView, version 5.0 (Statview, Abacus Concepts, Berkeley, CA, USA). Differences in the values at specific stages between the groups were assessed by one-way analysis of variance combined with Fisher's test. $p < 0.05$ was considered statistically significant. Survival curves were analysed by the Kaplan–Meier method and compared using log-rank tests.

Results

Pro-survival effect of systemic IL-10 in DS rats

Compared to the control EGFP transduction, IL-10 transduction significantly improved survival rates in DS

rats fed a high-sodium diet ($p < 0.001$, Figure 2). After 13 weeks of the gene delivery, serum IL-10 concentrations significantly increased in the IL-10-transduced rats compared to the normal untreated rats or control EGFP-transduced rats (986.6 ± 278.5 pg/ml versus <3 or 20.8 ± 18.1 pg/ml, $p < 0.001$, respectively; Figure 3). At this time point, the EGFP transduction generated a slight but significant increase of endogenous IL-10 levels compared to control ($p < 0.01$).

Anti-hypertensive effects of IL-10

SBP gradually increased in the EGFP group, resulting in levels of 184 ± 7 mmHg at 15 weeks of age (Figure 4). At 9 weeks (i.e. after 4 weeks of the vector injection), SBP in the IL-10 group (151 ± 7 mmHg) was significantly lower

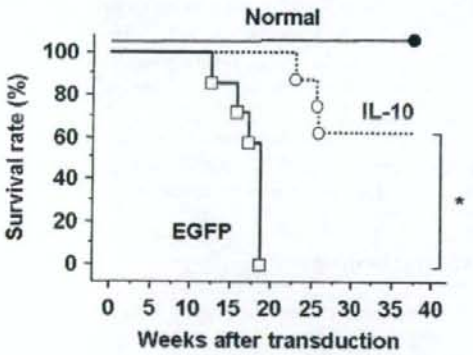

Figure 2. The pro-survival effects of IL-10 in DS rats. The 5-week-old rats were intramuscularly injected with AAV1-IL-10 or AAV1-EGFP at 1×10^{11} g.c./body. Kaplan–Meier survival analysis was performed. Closed circle, normal group; open circles, IL-10 group; open squares, EGFP group ($n = 8$ each). *$p < 0.001$ versus EGFP group

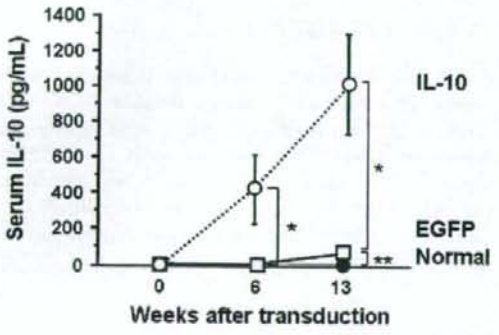

Figure 3. AAV vector-mediated systemic IL-10 expression in DS rats. AAV1-EGFP or AAV1-IL-10, at 1×10^{12} g.c./body, respectively, was injected bilaterally into the anterior tibial muscles of the 5-week-old rats. Serum IL-10 levels were determined periodically by ELISA. The normal group includes DS rats fed a low-sodium diet and not administered the vector injection. The results are presented as means ± SD ($n = 10$ each). *$p < 0.001$, **$p < 0.01$

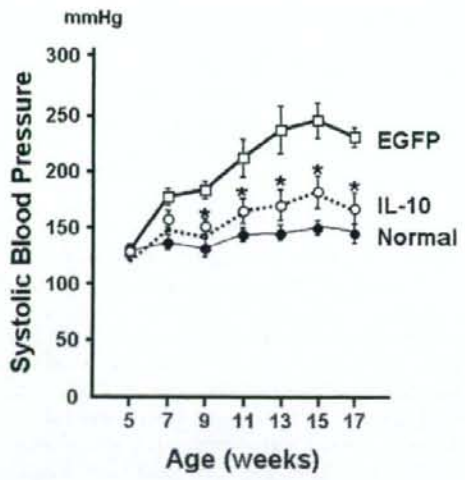

Figure 4. The anti-hypertensive effect of IL-10. Longitudinal tracing of systolic blood pressure evaluated by the tail-cuff method after injecting the AAV vectors in 5-week-old DS rats. Open squares, EGFP group; open circles, IL-10 group; closed circles, normal group ($n = 10$ each). The results are presented as means ± SD. *$p < 0.001$ versus EGFP group

Table 1. Effects of IL-10 on left ventricular hypertrophy and function

	RWT (mm)		%FS (%)	
Age (weeks)	5	11	5	18
Normal	0.46 ± 0.03	0.48 ± 0.02	58.7 ± 3.7	57.2 ± 3.9
EGFP	0.45 ± 0.03	0.63 ± 0.04*	59.8 ± 1.9	32.9 ± 4.4*
IL-10	0.45 ± 0.04	0.49 ± 0.02**	59.4 ± 2.6	59.2 ± 4.6**

M-mode echocardiograms of the LV at the papillary muscle level were traced for analysis. RWT of the LV as an index of LV hypertrophy and %FS as an index of systolic LV function were calculated as described in the Materials and methods. The results are presented as means ± SD ($n = 10$ each). *$p < 0.0001$ versus Normal group, **$p < 0.0001$ versus EGFP group at the same time-point, respectively.

than that in the EGFP group ($p < 0.0001$). The anti-hypertensive effect of IL-10 persisted until the animals were sacrificed at 18 weeks of age.

Effects of IL-10 on left ventricular hypertrophy, function and CHF

Echocardiography exhibited a 22.0% reduction in the RWT of the LV posterior wall at 11 weeks of age ($p < 0.0001$) and a 26.3% improvement in %FS of the LV wall at 18 weeks of age ($p < 0.0001$) in the IL-10 group compared to the EGFP group (Table 1). As compared to EGFP expression, IL-10 expression caused a 21.7% or 52.7% decrease in the heart or lung weight/body weight index, respectively (all $p < 0.05$; Figures 5a and 5b). Similarly, the cardiac ANP mRNA level significantly increased in the EGFP group compared to the control (46.5 ± 23.8-fold); whereas, IL-10 transduction significantly suppressed this increase (9.28 ± 5.2-fold) compared to control (Figure 5c).

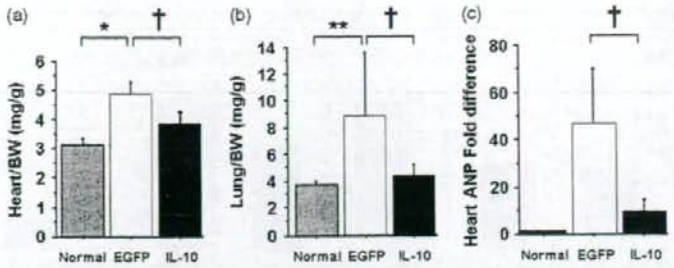

Figure 5. Effects of IL-10 on congestive heart failure. The hearts (a) and lungs (b) of DS rats were harvested and weighed at 18 weeks of age. Data were expressed after normalization using body weight. The cardiac ANP mRNA levels determined by real-time RT-PCR (c). The total RNA was extracted from the heart at 18 weeks of age. The mRNA levels were corrected by using the GAPDH mRNA level of each animal and then normalized to the mean value of the normal group. The results are presented as means ± SD ($n = 10$ each). *$p < 0.01$ versus Normal group, **$p < 0.05$ versus Normal group, †$p < 0.05$ versus EGFP

Effects of IL-10 on pathological cardiac remodelling

H&E staining demonstrated increased interstitial and perivascular cell infiltration in the failing heart of the EGFP-transduced rats (Figure 6a). Azan–Mallory staining demonstrated that interstitial and perivascular fibrosis increased in the EGFP group (Figure 6b). IL-10 transduction inhibited fibrosis and significantly decreased the cardiac TGF-β_1 levels in DS rats compared to the EGFP transduction (64.5 ± 45.3 pg/mg protein versus 197.1 ± 91.9 pg/mg protein, $p < 0.05$; Figure 6c).

Effects of IL-10 on renal function

Compared to control rats, DS rats fed a high-sodium diet exhibited a 68.0% increase in serum creatinine, a 243.0% increase in urine protein levels, and a 49.9% decrease in glomerular filtration rate (all $p < 0.05$; Figure 7). Sustained IL-10 expression reduced these changes by 88.2%, 100% and 45.8%, respectively (all $p < 0.05$).

Discussion

The present study demonstrates that systemic IL-10 expression via the AAV serotype 1 vector prevented the progression of hypertension, CHF and renal dysfunction in DS rats. A single intramuscular injection of AAV1-IL-10 achieved long-term systemic IL-10 expression, leading to the prolonged survival of the rats. The IL-10 transduction not only preserved systolic LV function, but also reduced fibrosis of the LV at the heart failure phase. The anti-hypertensive effect of IL-10 occurred prior to the

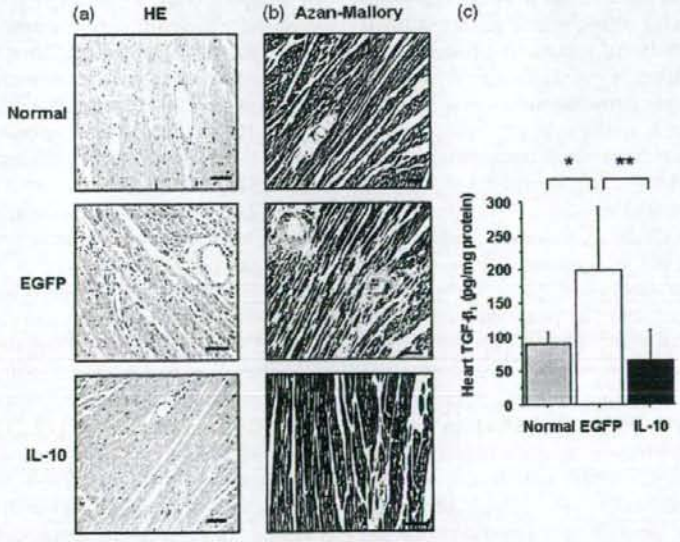

Figure 6. Histopathology and cardiac TGF-β_1 levels of the 18-week-old DS rats. (a) Representative micrographs of the H&E staining. (b) Representative micrographs of Azan–Mallory staining. Magnification, ×200; scale bar = 100 μm. (c) TGF-β_1 concentrations in the heart homogenates determined by ELISA. The results are presented as means ± SD ($n = 10$ each). *$p < 0.05$ versus Normal group, **$p < 0.05$ versus EGFP group

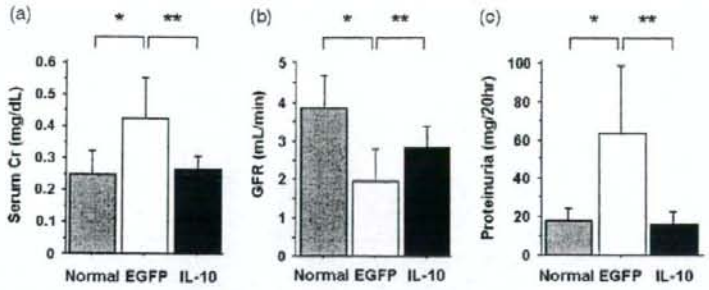

Figure 7. Effects of IL-10 on renal function in DS rats. (a) Serum creatinine (Cr), (b) glomerular filtration rate (GFR) and (c) urine protein levels were determined at 18 weeks of age. The results are presented as means ± SD ($n = 10$ each). *$p < 0.001$ versus Normal group, **$p < 0.05$ versus EGFP group

development of CHF and LVH, suggesting that this effect may largely contribute to amelioration of sodium-induced hypertensive organ damage.

Many studies have suggested the therapeutic potentials of IL-10 for CHF. Serum IL-10 levels decrease in CHF patients [19], and exogenous IL-10 administration retards progression of the disease in many cardiovascular disease models [20]. However, these studies used CHF models in which CHF was a result of acute viral or autoimmune myocarditis, and they examined the short-term IL-10 effects against initial inflammatory responses [11,12]. In the present study, we demonstrated the effects of long-term IL-10 expression against chronic CHF progression, hypertension and inflammatory changes of the cardiac tissue.

We detected a slight but significant increase of endogenous IL-10 levels in the heart failure phase in control DS rats. However, this increase was insufficient to cause beneficial effects. On the other hand, conventional IL-10 therapies based on recombinant drugs or plasmids require frequent administration for sufficient and sustained IL-10 expression. Thus, we used AAV vectors that permit long-term transgene expression *in vivo* [14]. Previously, we demonstrated that a single intramuscular injection of the AAV5-based vector caused systemic IL-10 expression for 1 year [21]. Since AAV1 is more efficient for muscle transduction than AAV2 or AAV5 [22], we used AAV1 as the vector in the present study [23].

A clinical trial using infliximab, a chimeric monoclonal antibody to TNF-α, failed to prolong the survival of CHF patients over the long term [5]. We speculate that the failure might be in part based on an insufficient regulation of the cytokine network, which may be involved in the progression of CHF and other related diseases such as hypertension and renal failure. Recent studies have shown the marked anti-hypertensive effects of an immunosuppressant mycophenolate mofetil (MMF) in DS rats [3,4]. MMF administration also ameliorates renal dysfunction via anti-inflammatory effects. Interestingly, an intramuscular injection of AAV1-IL-10 successfully ameliorated renal function in a rat model after nephrectomy [24]. We also observed that systemic IL-10 expression significantly attenuated hypertension and renal dysfunction, along with a decrease of inflammatory cell infiltration, in the kidney of stroke-prone spontaneously hypertensive rats (T. Nomoto *et al.*, unpublished data). In the present study, we demonstrate that IL-10 gene therapy successfully ameliorated heart failure and renal dysfunction along with a suppression of severe hypertension in DS rats. These observations suggest that anti-inflammatory action of IL-10 may attenuate the target organ damage related to high blood pressure. However, precise mechanism underlying the anti-hypertensive effect of IL-10 require further investigation.

The synthesis of ANP, a cardioprotective hormone predominantly produced by the ventricle, as well as its circulating levels, increases in accordance with the severity of CHF [25,26]. Administration of exogenous ANP ameliorates CHF in clinical settings via its diuretic and vasodilatory effects. In the present study, the cardiac ANP mRNA level significantly decreased in the IL-10 group. These observations suggest that IL-10 ameliorated CHF independently of direct ANP production but inhibited the adaptive increase in ANP levels.

The present study demonstrates that IL-10 expression attenuated pathological cardiac remodelling with reduced expression of TGF-β_1, a hallmark of cardiac fibrosis in DS rats [27]. Expression of monocyte chemoattractant protein (MCP)-1 in the endothelium of intramyocardial arterioles triggers perivascular macrophage accumulation [28]. Macrophage infiltration induces TGF-β_1 production, leading to fibroblast proliferation and extracellular matrix production [29]. Interestingly, a neutralizing antibody against TGF-β inhibits fibroblast activation, resulting in reduced collagen production and subsequent myocardial fibrosis [30]. Previously, we reported that systemic IL-10 expression significantly decreased serum MCP-1 levels, perivascular macrophage infiltration, and pulmonary tissue TGF-β_1 levels *in vivo* [10,21]. These observations suggest that the reduced macrophage-derived TGF-β_1 expression following MCP-1 suppression might be responsible for the anti-remodelling effects of IL-10. However, the direct effects of IL-10 on TGF-β_1 in the pathogenesis of CHF remain unclear.

Epidemiological studies have demonstrated that the increased pro-inflammatory cytokine expression is related to the incidence of pre-hypertension [31]. These results

suggest a possible link between the inflammatory response and the development of hypertension. This is the first study to demonstrate the anti-hypertensive effects of IL-10, which might be a key molecule to explain this relationship. Exploring the mechanisms underlying the effects of IL-10 would provide new molecular targets for refractory hypertension and its sequalae.

In conclusion, the sustained IL-10 expression achieved by the single AAV-IL-10 injection ameliorated CHF and prolonged survival in DS rats. IL-10 expression attenuated salt-sensitive hypertension, LV remodelling and renal dysfunction. These results suggest that our IL-10-based strategy potentially prevents the progression of refractory hypertensive organ damage in humans.

Acknowledgements

We thank Miyoko Mitsu and Takako Takagi for their encouragement and technical support. This work was supported by grants from the Ministry of Health, Labour and Welfare of Japan. This work was also supported by Grants-in-Aid for Scientific Research; a grant from the 21 Century COE program; and High-Tech Research Centre Project for Private Universities, matching fund subsidy, from the Ministry of Education, Culture, Sports, Science and Technology of Japan; and a research award to Jichi Medical School Graduate Student. This work was performed at Jichi Medical University in Shimotuke-shi, Tochigi, Japan.

References

1. Levine B, Kalman J, Mayer L, *et al.* Elevated circulating levels of tumor necrosis factor in severe chronic heart failure. *N Engl J Med* 1990; **323**: 236–241.
2. Vasan RS, Sullivan LM, Roubenoff R, *et al.* Inflammatory markers and risk of heart failure in elderly subjects without prior myocardial infarction: the Framingham Heart Study. *Circulation* 2003; **107**: 1486–1491.
3. Mattson DL, James L, Berdan EA, *et al.* Immune suppression attenuates hypertension and renal disease in the Dahl salt-sensitive rat. *Hypertension* 2006; **48**: 149–156.
4. Tian N, Gu JW, Jordan S, *et al.* Immune suppression prevents renal damage and dysfunction and reduces arterial pressure in salt-sensitive hypertension. *Am J Physiol Heart Circ Physiol* 2007; **292**: H1018–H1025.
5. Chung ES, Packer M, Lo KH, *et al.* Randomized, double-blind, placebo-controlled, pilot trial of infliximab, a chimeric monoclonal antibody to tumor necrosis factor-alpha, in patients with moderate-to-severe heart failure: results of the anti-TNF Therapy Against Congestive Heart Failure (ATTACH) trial. *Circulation* 2003; **107**: 3133–3140.
6. Mann DL, McMurray JJ, Packer M, *et al.* Targeted anticytokine therapy in patients with chronic heart failure: results of the Randomized Etanercept Worldwide Evaluation (RENEWAL). *Circulation* 2004; **109**: 1594–1602.
7. Elenkov IJ, Chrousos GP. Stress hormones, proinflammatory and antiinflammatory cytokines, and autoimmunity. *Ann NY Acad Sci* 2002; **966**: 290–303.
8. Cattaruzza M, Slodowski W, Stojakovic M, *et al.* Interleukin-10 induction of nitric-oxide synthase expression attenuates CD40-mediated interleukin-12 synthesis in human endothelial cells. *J Biol Chem* 2003; **278**: 37874–37880.
9. Selzman CH, McIntyre RC, Jr., Shames BD, *et al.* Interleukin-10 inhibits human vascular smooth muscle proliferation. *J Mol Cell Cardiol* 1998; **30**: 889–896.
10. Ito T, Okada T, Miyashita H, *et al.* Interleukin-10 expression mediated by an adeno-associated virus vector prevents monocrotaline-induced pulmonary arterial hypertension in rats. *Circ Res* 2007; **101**: 734–741.
11. Nishio R, Matsumori A, Shioi T, *et al.* Treatment of experimental viral myocarditis with interleukin-10. *Circulation* 1999; **100**: 1102–1108.
12. Palaniyandi SS, Watanabe K, Ma M, *et al.* Inhibition of mast cells by interleukin-10 gene transfer contributes to protection against acute myocarditis in rats. *Eur J Immunol* 2004; **34**: 3508–3515.
13. Kihara Y, Sasayama S. Transition from compensatory hypertrophy to dilated failing left ventricle in Dahl-Iwai salt-sensitive rats. *Am J Hypertens* 1997; **10**: 78S–82S.
14. Okada T, Shimazaki K, Nomoto T, *et al.* Adeno-associated viral vector-mediated gene therapy of ischemia-induced neuronal death. *Methods Enzymol* 2002; **346**: 378–393.
15. Matsushita T, Elliger S, Elliger C, *et al.* Adeno-associated virus vectors can be efficiently produced without helper virus. *Gene Ther* 1998; **5**: 938–945.
16. Okada T, Nomoto T, Yoshioka T, *et al.* Large-scale production of recombinant viruses by use of a large culture vessel with active gassing. *Hum Gene Ther* 2005; **16**: 1212–1218.
17. Nakahara T, Hashimoto K, Hirano M, *et al.* Acute and chronic effects of alcohol exposure on skeletal muscle c-myc, p53, and Bcl-2 mRNA expression. *Am J Physiol Endocrinol Metab* 2003; **285**: E1273–1281.
18. Ueno S, Ohki R, Hashimoto T, *et al.* DNA microarray analysis of in vivo progression mechanism of heart failure. *Biochem Biophys Res Commun* 2003; **307**: 771–777.
19. Stumpf C, Lehner C, Yilmaz A, *et al.* Decrease of serum levels of the anti-inflammatory cytokine interleukin-10 in patients with advanced chronic heart failure. *Clin Sci (Lond)* 2003; **105**: 45–50.
20. Ito T, Ikeda U. Inflammatory cytokines and cardiovascular disease. *Curr Drug Targets Inflamm Allergy* 2003; **2**: 257–265.
21. Yoshioka T, Okada T, Maeda Y, *et al.* Adeno-associated virus vector-mediated interleukin-10 gene transfer inhibits atherosclerosis in apolipoprotein E-deficient mice. *Gene Ther* 2004; **11**: 1772–1779.
22. Hauck B, Chen L, Xiao W. Generation and characterization of chimeric recombinant AAV vectors. *Mol Ther* 2003; **7**: 419–425.
23. Ito T, Okada T, Mimuro J, *et al.* Adenoassociated virus-mediated prostacyclin synthase expression prevents pulmonary arterial hypertension in rats. *Hypertension* 2007; **50**: 531–536.
24. Mu W, Ouyang X, Agarwal A, *et al.* IL-10 suppresses chemokines, inflammation, and fibrosis in a model of chronic renal disease. *J Am Soc Nephrol* 2005; **16**: 3651–3660.
25. Saito Y, Nakao K, Arai H, *et al.* Augmented expression of atrial natriuretic polypeptide gene in ventricle of human failing heart. *J Clin Invest* 1989; **83**: 298–305.
26. de Boer RA, Henning RH, Suurmeijer AJ, *et al.* Early expression of natriuretic peptides and SERCA in mild heart failure: association with severity of the disease. *Int J Cardiol* 2001; **78**: 5–12.
27. Ichihara S, Obata K, Yamada Y, *et al.* Attenuation of cardiac dysfunction by a PPAR-alpha agonist is associated with down-regulation of redox-regulated transcription factors. *J Mol Cell Cardiol* 2006; **41**: 318–329.
28. Kuwahara F, Kai H, Tokuda K, *et al.* Hypertensive myocardial fibrosis and diastolic dysfunction: another model of inflammation? *Hypertension* 2004; **43**: 739–745.
29. Border WA, Noble NA. Transforming growth factor beta in tissue fibrosis. *N Engl J Med* 1994; **331**: 1286–1292.
30. Kuwahara F, Kai H, Tokuda K, *et al.* Transforming growth factor-beta function blocking prevents myocardial fibrosis and diastolic dysfunction, in pressure-overloaded rats. *Circulation* 2002; **106**: 130–135.
31. Chrysohoou C, Pitsavos C, Panagiotakos DB, *et al.* Association between prehypertension status and inflammatory markers related to atherosclerotic disease: the ATTICA Study. *Am J Hypertens* 2004; **17**: 568–573.

Hepatol Int (2008) 2:80–88
DOI 10.1007/s12072-007-9042-1

ORIGINAL ARTICLE

Adeno-associated virus vector-mediated production of hepatocyte growth factor attenuates liver fibrosis in mice

Kazuhiro Suzumura · Tadamichi Hirano · Gakuhei Son · Yuji Iimuro · Hiroaki Mizukami · Keiya Ozawa · Jiro Fujimoto

Received: 5 July 2007 / Accepted: 17 October 2007 / Published online: 22 December 2007

Abstract
Purpose Adeno-associated virus (AAV) vectors can achieve long-term gene expression and are now feasible for use in human gene therapy. We constructed hepatocyte growth factor (HGF) expressing AAV (AAV5-HGF) and examined its effect in two mouse hepatic fibrosis models.
Methods A model of hepatic fibrosis was established by carbon tetrachloride (CCl_4) administration in Balb/c mice. After the establishment of liver fibrosis, AAV5-HGF was injected once into the portal vein. Mice were killed 3, 6, 9, and 12 weeks after injection. Another model was established by bile duct ligation (BDL). Seven weeks after AAV5-HGF injection, mice underwent BDL, and were then killed 2 weeks after BDL.
Results Mice that received AAV5-HGF achieved stable HGF expression both in the serum and liver for at least 12 weeks. In both models, significant improvement of the liver fibrosis was found in all mice receiving AAV5-HGF based on Azan-Mallory staining. Suppression of hepatic stellate cells (HSC) was confirmed by immunohistochemistry. Fibrogenic markers were significantly suppressed and collagenase activity increased in the livers of mice receiving AAV5-HGF.
Conclusions A single injection of AAV vector containing HGF gene achieved long-term expression of HGF and resulted in resolution of mouse liver fibrosis. HGF gene therapy mediated by AAV is feasible for the treatment of liver fibrosis.

Keywords HGF · Liver fibrosis · AAV · CCl_4 · BDL

Abbreviations

AAV	Adeno-associated virus
BDL	Bile duct ligation
CCl_4	Carbon tetrachloride
HGF	Hepatocyte growth factor

Introduction

Liver fibrosis is induced by the wound healing response to chronic liver injury caused by hepatitis virus infections, alcohol abuse, prolonged biliary obstruction, hepatotoxic drugs, or metabolic diseases [1]. It is a major cause of morbidity and mortality worldwide, with no effective therapy except for liver transplantation. The main characteristic of liver fibrosis is the excess production and deposition of extracellular matrix (ECM) caused by activated hepatic stellate cells (HSC), portal fibroblasts, and myofibroblasts of bone marrow origin. These cells are activated by fibrogenic cytokines, like transforming growth factor (TGF)-β [2]. Liver fibrosis was considered to be an irreversible end result, but recent studies have demonstrated that liver fibrosis is reversible after clearance of hepatitis C virus (HCV) with either interferon or pegylated interferon, with or without the addition of ribavirin [3–6]. These reports demonstrate the reversibility of human liver fibrosis.

K. Suzumura · T. Hirano · G. Son · Y. Iimuro · J. Fujimoto (✉)
First Department of Surgery, Hyogo College of Medicine, 1-1 Mukogawacho, Nishinomiya, Hyogo 663-8501, Japan
e-mail: sfujimo@hyo-med.ac.jp

H. Mizukami · K. Ozawa
Division of Genetic Therapeutics, Center for Molecular Medicine, Jichi Medical University, Shimotsuke, Tochigi 329-0498, Japan

Prior to these reports, the in vivo therapeutic effect of hepatocyte growth factor (HGF) against liver fibrosis was shown. The HGF identified and cloned as a 69-kDa α-chain and a 34-kDa β-chain, initially was characterized as a potent mitogen for hepatocytes [7, 8]. HGF also shows mitogenic, motogenic, and morphogenic activities in a wide variety of cell types [9]. Several in vivo approaches have shown that HGF plays an essential role in both the development and regeneration of liver [10] and have demonstrated antiapoptotic and cytoprotective effects in hepatocytes [11]. The first report demonstrating the effect of HGF on liver fibrosis used recombinant HGF injection [12]. However, a large amount of recombinant HGF was required, because HGF is unstable in blood, with a half-life of 3–5 min [13, 14]. In order to overcome this problem, we demonstrated HGF gene therapy using hemagglutinating virus of Japan (HVJ) liposomes [15]. The HGF gene transfection into rat skeletal muscle dramatically improves liver fibrosis; however, this strategy also requires repetitive transfections to achieve persistent expression because HVJ-liposome-mediated gene expression is transient [16]. From a clinical point of view, development of a novel gene transfer strategy to achieve long-term expression of HGF protein in vivo is crucial. Therefore, we assessed the therapeutic efficacy of adeno-associated virus (AAV) vector-mediated HGF gene therapy for liver fibrosis.

AAV includes a number of small single-stranded DNA viruses and members of the parvovirus family. A number of unique properties make AAV a very promising vector for gene therapy. The advantages of the use of AAV-based vectors are that they can transduce therapeutic genes into both dividing and nondividing cells and achieve long-term gene expression with no apparent adverse effect [17, 18]. In this study, we constructed a recombinant AAV vector coding the human HGF gene (AAV-HGF) and assessed its therapeutic effects for hepatic fibrosis using two mouse models of hepatic fibrosis.

Materials and methods

Cell culture

The human HCC cell line, HepG2, was grown in Dulbecco modified Eagle medium (DMEM) with 10% fetal bovine serum (FBS), 100 U/ml penicillin, and 100 mg/ml streptomycin.

Animals

Male Balb/c mice (6-week-old) were purchased from Japan CLEA, and were maintained in a pathogen-free facility at Hyogo College of Medicine (Nishinomiya, Hyogo, Japan). The animal experiments were performed in accordance with the guidelines of the National Institutes of Health (Bethesda, MD, U.S.A.), as specified by the animal care policy of Hyogo College of Medicine.

Plasmid AAV5-HGF construction

We first evaluated vectors derived from AAV serotypes 1, 2, and 5. LacZ gene expression recombinant AAV vectors (AAV1-LacZ, AAV2-LacZ, or AAV5-LacZ) were transduced into mouse livers using the same method described below, and efficiency of gene expression was determined by LacZ staining. Among these vectors, AAV5-LacZ had the highest LacZ expression (unpublished result). On the basis of this result, we selected the AAV serotype 5 for the present study and constructed the AAV5-HGF vector. Plasmid AAV5-HGF was constructed by inserting the full-length cDNA of human HGF [19], representing about 2.2 kb, at the Hinc II site of the AAV5-MCS that included the CMV promoter and inverted terminal repeat sequence.

AAV5-HGF vector preparation

Plasmids for AAV vector production were purchased from Stratagene (La Jolla, CA, USA). pAAV5-CMV-LacZ, a plasmid encoding LacZ, and 5RepCapA, a helper plasmid for AAV serotype 5, were generous gifts from Dr J. A. Chiorini (National Institutes of Health, Bethesda, MD, USA) [20]. pAAV5-CMV-HGF containing the HGF sequence was prepared as previously described, with the inverted terminal repeat (ITR) sequences changed to those of the AAV5 vector. Recombinant AAV vector stocks were prepared in accordance with an adenovirus-free triple-plasmid transfection protocol [21]. After harvest, vector solutions were purified twice on a cesium chloride (CsCl) gradient and quantified by DNA dot blot hybridization. The same vector stock was used in the same series of experiments to minimize the variability that could occur as a result of the potential differences in vector potency.

AAV vector transduction in vitro

In order to confirm HGF expression in vitro, HepG2 cells (2×10^5) were plated in 6-cm plastic dishes. After 24 h, cells were infected with 10^6 or 2×10^6 vector genomes of AAV5-HGF. Forty-eight hours after transduction, culture medium and cell lysates were harvested. AAV5-LacZ was transfected into HepG2 cells using the same procedure as that for a control vector. Protein concentrations of human